Charge-transfer cross sections in collisions of ground-state Na atoms with H^+ at low-eV collision energies

C. M. Dutta,[1] P. Nordlander,[1] M. Kimura,[2] and A. Dalgarno[3]
[1]*Department of Physics and Rice Quantum Institute, Houston, Texas 77251-1892*
[2]*Graduate School of Science and Engineering, Yamaguchi University, Ube, Yamaguchi 755, Japan*
[3]*Harvard-Smithsonian Center for Astrophysics, Cambridge, Massachusetts 02138*
(Received 26 June 2000; published 12 January 2001)

Cross sections for nonradiative charge transfer in $H^+ + Na(3s)$ collisions at energies less than or equal to 40 eV have been calculated using a fully quantum-mechanical approach. The calculated cross sections agree well with the experimental data in the entire energy range, but do not agree with other calculations at low energies. We discuss possible causes of this difference. Using the calculated cross sections, the rate coefficients at temperatures below 20 000 K have been calculated, and compared with those of other theoretical calculations.

DOI: 10.1103/PhysRevA.63.022709 PACS number(s): 34.70.+e

I. INTRODUCTION

The distribution of sodium between its ionized and neutral stages is important to interpretations of observations of the resonance line of sodium atoms in the atmospheres of the planets and comets [1] and the interstellar medium where small scale fluctuations have been detected that may in part reflect changes in the balance between neutral and ionized sodium [2–6]. Charge transfer between sodium ions and neutral hydrogen atoms and between neutral sodium atoms and protons may modify the ionization distribution also in stellar winds [6]. Charge-transfer processes at energies of the order of 100 eV are significant in determining the ionization structure of the edge regions of thermonuclear fusion plasmas.

Charge transfer in collisions of ground-state Na atoms with protons has been studied extensively both theoretically [7,8,10–12,9,13–15] and experimentally [16–20,9]. However, most of the earlier studies were carried out at keV collision energies. A few studies have been performed in the eV region. Allan [7] calculated the cross section at 22 eV using the semiclassical impact-parameter method, and Croft and Dickinson [14] carried out fully quantum-mechanical calculations of nonradiative charge-transfer cross sections for energies below 40 eV. Kushawaha [18] measured nonradiative charge-transfer cross sections at energies 1.5–600 eV. In the present work, we have carried out fully quantum-mechanical calculations of nonradiative charge-transfer cross sections for $Na(3s)$ colliding with H^+, namely, $Na(3s) + H^+ \rightarrow Na^+ + H\ (n=2) - 1.682$ eV at energies below 40 eV. Using the calculated cross sections, we have calculated the rate coefficients for temperatures below 20 000 K. Our calculated charge-transfer cross sections agree well with experimental data [18], but are found to be different from the results calculated by Croft and Dickinson [14]. In Sec. II we describe our theoretical approach. In Sec. III we present our calculated charge-transfer cross sections and the rate coefficients, and compare with experimental data. We also analyze possible causes of the difference between the two calculations. Conclusions are given in Sec. IV.

II. THEORY

We calculated the charge-transfer cross section, by coupling the six molecular states and counting from the second lowest state $2\ ^2\Sigma$, $3\ ^2\Sigma$, $4\ ^2\Sigma$, $5\ ^2\Sigma$, $1\ ^2\Pi$, and $2\ ^2\Pi$, of the NaH^+, which separate, respectively, to $Na(3s)+H^+$, $Na^+ + H(2p\sigma^+)$, $Na^+ + H(2p\sigma^-)$, $Na(3p\sigma)+H^+$, $Na^+ + H(2p\pi)$, and $Na(3p\pi)+H^+$. $H(2p\sigma^{\pm})$ denotes the Stark-split hydrogen $n=2$ orbitals in the presence of a single charge. The same set of states was used in the calculations by Croft and Dickinson [14].

The molecular potentials and molecular orbitals were obtained using the configuration-interaction (CI) method in which the Na^+ core was represented by the pseudopotential given by Bardsley [21]. The molecular orbitals are represented by a linear combination of Slater orbitals chosen as a basis set. The Slater orbitals and their exponents used here are listed in Table I. The lowest $[Na^+ + H(1s):1\ ^2\Sigma]$ state lies about 8 eV below the initial $[Na(3s)+H^+:2\ ^2\Sigma]$ state. This state becomes important for radiative charge transfer for kinetic energies below a few eV, but may be excluded for nonradiative charge transfer. The next higher state above the

TABLE I. Slater orbitals and exponents.

Site	Σ states STO	Exponent	Π states STO	Exponent
H site	$1s$	2.0000	$2p$	1.0000
		1.0000		0.5000
		0.5000		0.3333
	$2s$	0.5000	$3d$	0.3333
		0.3333		
	$2p$	1.0000		
		0.5000		
		0.3333		
	$3d$	0.3333		
Na site	$2s$	0.7900	$3p$	0.7210
	$3s$	2.4870		0.5580
		0.6940	$3d$	0.3370
		0.3720		1.484
	$3p$	0.7210		
		0.5580		
	$3d$	0.3350		
		0.6700		
	$4s$	0.2900		

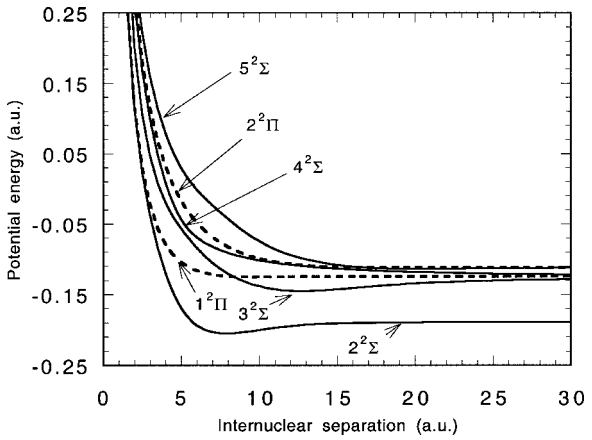

FIG. 1. Adiabatic potentials for HNa^+. Solid lines correspond to the Σ states, $2\ ^2\Sigma$, $3\ ^2\Sigma$, $4\ ^2\Sigma$, and $5\ ^2\Sigma$, respectively, counting from low energies. The dashed lines represent the $1\ ^2\Pi$ and $2\ ^2\Pi$ states, respectively.

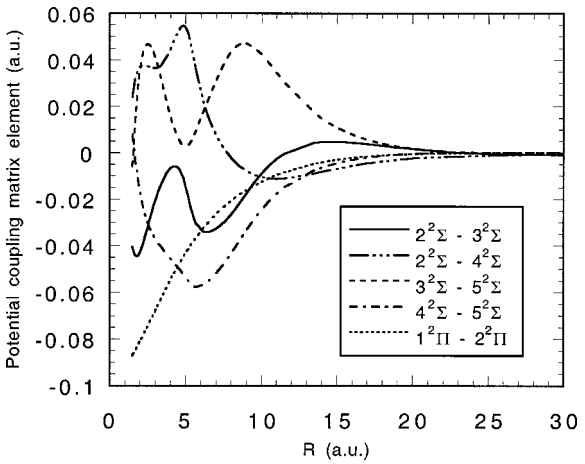

FIG. 2. The potential coupling matrix elements of the present work.

$2\ ^2\Pi$ state, the $[\mathrm{Na}(4s)+\mathrm{H}^+;\ 6\ ^2\Sigma]$ state, lies about 1.09 eV above the $2\ ^2\Pi$ state. This and other higher states are also excluded. The radial and rotational coupling matrix elements were obtained numerically. The present approach uses the atomic plane-wave-type electron translation factors (ETF's), while Croft and Dickinson used the so-called reaction coordinates given by Thorson and Delos [22] which involved a different form of ETF. The nuclear wave functions were expanded into partial waves. For computational convenience, these six states were transformed to the so-called diabatic states [23] in order to eliminate the first derivatives of the internuclear separation R in the close-coupled differential equations. The coupled equations were solved using the logarithm-derivative method [24], with integrations carried out with the internuclear separation R from 1.5 to 70 a.u.

The rate coefficient Γ for the charge-transfer process was calculated from the cross sections, using

$$\Gamma = \int_0^\infty v\,\sigma(v) f(v,T)\,dv \tag{1}$$

where v is the velocity of the incoming particle, T is temperature, and $f(v,T)$ is the Maxwell-Boltzmann velocity distribution function. The calculated cross sections were spline fitted and interpolated for the numerical integration of Eq. (1).

III. RESULTS AND DISCUSSION

Figure 1 shows the adiabatic potential energies of the six molecular states that were included in our coupled state calculations. The full lines and dotted lines represent the $^2\Sigma$ and $^2\Pi$ states, respectively. There is an avoided crossing between the $3\ ^2\Sigma$ and $4\ ^2\Sigma$ states at $R\sim 5$ a.u. and a broad weak avoided crossing between $2\ ^2\Sigma$ and $3\ ^2\Sigma$ at $R\sim 12$ a.u. The energies of these states calculated at the internuclear distance, $R=150$ a.u., were found to agree better than 0.1% with the spectroscopic data [25], except the $2\ ^2\Pi$ state which was within 0.6%. Figure 2 shows our potential coupling matrix elements between the different states. Here, the potential coupling matrix is defined as $\mathbf{C}^{-1}\boldsymbol{\epsilon}\mathbf{C}$, where the matrix $\mathbf{C}$ is the matrix which is used to eliminate the first derivative of the wave function [23], and $\boldsymbol{\epsilon}$ is the eigenvalue matrix, respectively. Since the energy as well as the $\mathbf{C}$ matrix, which depends on the complete model, are involved, an unambiguous comparison of our potential coupling with those shown in [14] is not possible. Among our potential coupling matrix elements connecting the incoming $2\ ^2\Sigma$ channel with the charge-transfer channels, the one with $4\ ^2\Sigma$ is larger than the one with $3\ ^2\Sigma$ at smaller R, but their magnitudes become comparable at larger R. Figures 3(a)–3(d) compare the rotational coupling matrix elements in the present work with those used by Croft and Dickinson. From Fig. 3(a), it is seen that the rotational coupling matrix element between the incoming $2\ ^2\Sigma$ channel and the charge-transferred $1\ ^2\Pi$ state is significant for R up to $\sim$20 a.u. and larger than the potential and rotational coupling matrix elements which directly couple the initial channel to the other charge-transfer states, $3\ ^2\Sigma$ and $4\ ^2\Sigma$. Therefore, we expect large contributions to the charge-transfer cross section from the $1\ ^2\Pi$ partial cross section. The rotational coupling matrix elements between $2\ ^2\Sigma$ and $2\ ^2\Pi$ are relatively large, but they do not lead to charge transfer. Comparing our results with those in Ref. [14], there are differences in magnitude, but the overall shapes are similar.

In order to test our basis set and coupling matrix elements, we carried out semiclassical impact-parameter calculations of charge-transfer cross sections in the energy region between 0.5 and 2 keV/u. Figure 4 compares the results with those for H $(n=2)$ calculated by Fritsch [11]. Our charge-transfer cross sections agree very well with the overall trend. The magnitudes of our cross sections are about 70% of those of Fritsch. This is understandable since the basis set of Fritsch includes Slater orbitals of all H $(n=1-3)$ and 12 Slater-type orbitals at the Na center to represent the Na($3s$, $3p$, and $3d$) orbitals. Because we are interested in very low energies, the basis set we used should be adequate.

Figure 5 compares charge-transfer cross sections obtained

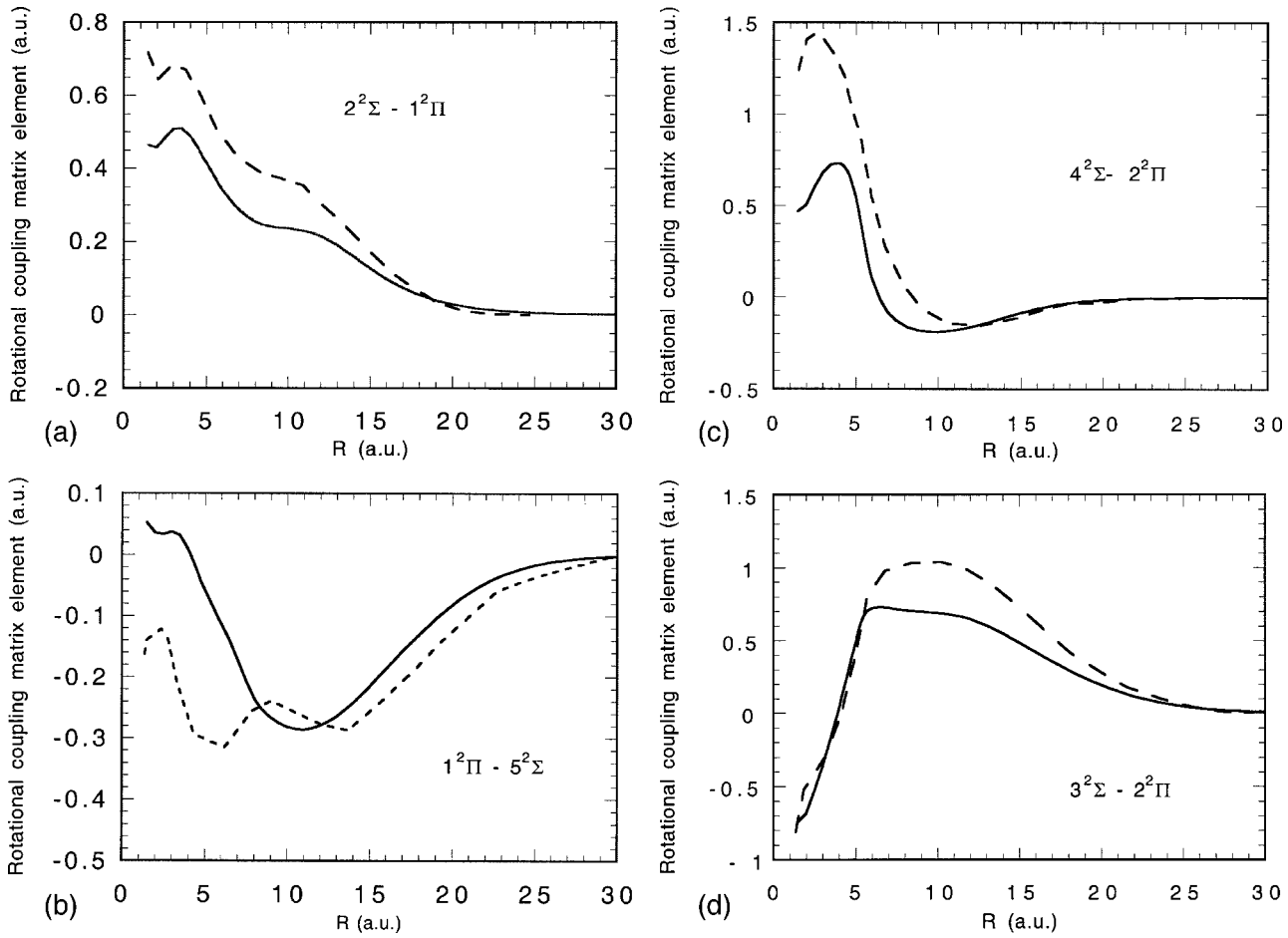

FIG. 3. Comparison of the rotational coupling matrix elements of the present calculation (full lines) with those by Ref. [14] (dashed lines).

here with experimental data [18] and with cross sections calculated by Croft and Dickinson [14]. Our results are in very good agreement with the experiment, except at the lowest kinetic energy point, where the experimental error bar is large. The theoretical results by Croft and Dickinson are larger than the measurements at higher energies, but are smaller by three order of magnitude for energies near 2 eV. The major difference between our total charge-transfer cross sections and those by Croft and Dickinson comes from the partial cross section of the 1 $^2\Pi$ state, as seen in Fig. 6. In

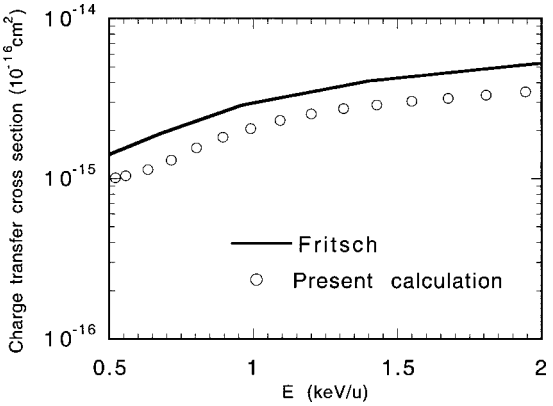

FIG. 4. Comparison of the charge-transfer cross sections computed using the semiclassical impact-parameter method. The solid line is by Fritsch [11], and the circles are the values calculated in the present work.

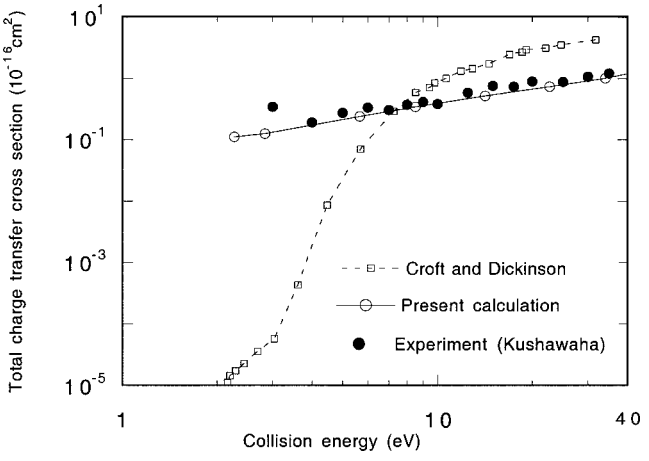

FIG. 5. Comparison of the charge-transfer cross sections. The open circles connected by the full line are from the present work, and the open squares connected by the dashed line are from Ref. [14]. The experimental data of Ref. [18] are shown by the filled circles.

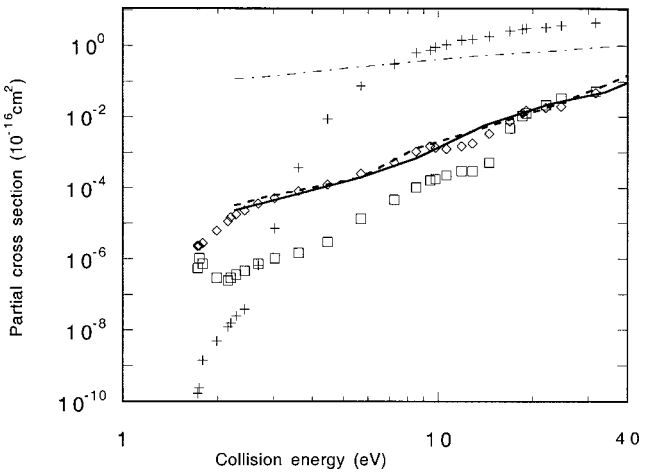

FIG. 6. Comparison of partial cross sections calculated by the present work with those by Ref. [14]. In the present work, the dotted line represents the 3 $^2\Sigma$ partial cross section, the full line the 4 $^2\Sigma$ partial cross section, and the dash-dot line the 1 $^2\Pi$ partial cross section. The partial cross sections for 3 $^2\Sigma$, 4 $^2\Sigma$, and 1 $^2\Pi$ of Ref. [14] are given by the symbols of diamond (3 $^2\Sigma$), square (4 $^2\Sigma$), and plus (1 $^2\Pi$).

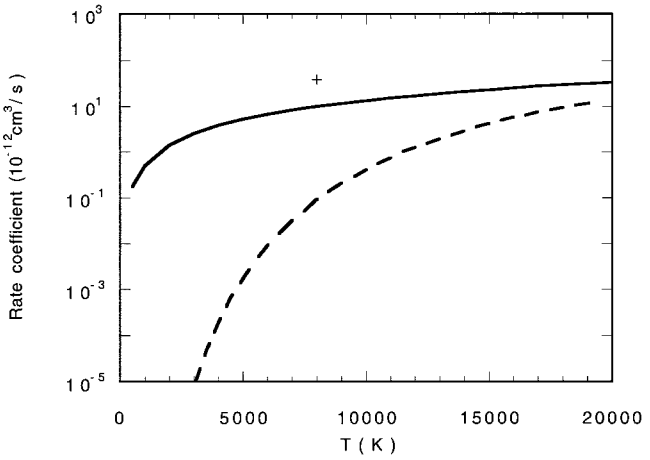

FIG. 7. Comparison of the rate coefficients. The full line is the present work, the dotted line is from Ref. [14], and + is from Ref. [6].

both calculations, at higher energies, the charge-transfer cross sections are dominated by the contributions from the 1 $^2\Pi$ channel. However, in the calculation of Croft and Dickinson, the 1 $^2\Pi$ contribution rapidly decreases as the collision energy decreases, whereas in the present calculation it does not. One might expect the effect of rotational coupling to decrease as the collision velocity decreases. However, our rotational coupling matrix element between the 1 $^2\Pi$ state and the initial 2 $^2\Sigma$ state extends to relatively large R values, and at very low energies the contribution from large R becomes increasingly significant. We also note that in our calculation the partial cross sections of the 3 $^2\Sigma$ and 4 $^2\Sigma$ states have nearly the same magnitude over the entire energy range. In order to understand the cause of this discrepancy, we carried out two-state (2 $^2\Sigma$ and 1 $^2\Pi$) coupled calculation at 2.7 eV, and found that the cross section that resulted was twice as large as that of the six state calculation. Addition of the 2 $^2\Pi$ state reduced the cross section by 16%, but the remaining reduction of the 1 $^2\Pi$ partial cross section must come mostly from the non-charge-transfer excited states via the indirect couplings. This involves complicated multistep processes and its elucidation by numerical calculation is difficult. Although our calculated total charge cross sections agree very well with the experimental data of Kushawaha [18], measurements at very low energies are difficult, and further experimental and theoretical studies would be helpful in reaching a definite conclusion on the low-energy behavior of the charge-transfer cross sections. Figure 7 shows the rate coefficients calculated using our charge-transfer cross sections, together with those by Croft and Dickinson and also by Natta and Giovanardi [6]. Our rate coefficients are larger than those by Croft and Dickinson, and the difference increases rapidly as the temperature decreases because of our larger charge-transfer cross sections at lower energies. The rate coefficient at $T=8000$ K by Natta and Giovanardi [6] was obtained using the cross sections measured by Kushawaha [18]. Since our calculated cross sections are slightly smaller than the measured values, our rate coefficient at $T=8000$ K is smaller than that of Natta and Giovanardi [6].

IV. CONCLUSION

We have carried out fully quantum-mechanical calculations of nonradiative charge-transfer cross sections for the process, $\mathrm{Na}(3s)+\mathrm{H}^+\rightarrow\mathrm{Na}^+ +\mathrm{H}\ (n=2)$. Our results for the cross sections agree well with the available experimental measurements, but differ from the cross sections calculated by Croft and Dickinson. The difference comes mainly from the 1 $^2\Pi$ partial cross sections. In the calculation of Croft and Dickinson, the 1 $^2\Pi$ partial cross section, which dominates other partial cross sections at higher energies, drops rapidly as the collision energy decreases. In contrast, our 1 $^2\Pi$ partial cross section remains dominant over the entire energy range. Further theoretical and experimental investigations are needed before reaching a conclusion on the low-energy behavior of the cross section. Using the calculated cross sections we obtained rate coefficients for charge transfer at temperature below 20 000 K and compared the results with earlier work.

ACKNOWLEDGMENTS

The work was supported in part by the grant-in-Aid, Ministry of Education, Science and Culture, Japan and The Japan Society for Promotion of Science (M.K.), and by the Robert A. Welch Foundation (P.N. and C.M.D.), by the National Science Foundation through Grant No. INT-9911858 (P.N. and C.M.D.), and a grant to the Institute for Theoretical Atomic and Molecular Physics at Harvard University and Smithsonian Astrophysical Observatory (M.K.), and by the Department of Energy, Office of Basic Energy Sciences (A.D.).

[1] *The Photochemistry of Atmospheres, Earth, the Other Planets and Comets*, edited by J. S. Levine (Academic Press, New York, 1985).
[2] G. E. Langer, C. F. Prosser, and C. Sneden, Astron. J. **100**, 216 (1990).
[3] D. M. Meyer and J. T. Lauroesch, Astrophys. J. Lett. **520**, L103 (1999).
[4] J. K. Watson and D. M. Meyer, Astrophys. J. Lett. **473**, L127 (1996).
[5] J. T. Lauroesch and D. M. Meyer, Astrophys. J. Lett. (to be published).
[6] A. Natta and C. Giovanardi, Astrophys. J. **356**, 646 (1990).
[7] R. J. Allan, J. Phys. B **19**, 321 (1986).
[8] C. Kubach and V. Sidis, Phys. Rev. A **23**, 110 (1981).
[9] T. Royer, J. Pommier, D. Dowek, N. Andersen, and J. C. Houver, Z. Phys. D: At., Mol. Clusters **10**, 45 (1988).
[10] M. Kimura, R. E. Olson, and J. Pascale, Phys. Rev. A **26**, 3113 (1982).
[11] W. Fritsch, Phys. Rev. A **30**, 1135 (1984).
[12] R. Shingal and B. H. Bransden, J. Phys. B **20**, 4815 (1987).
[13] C. Courbin, R. J. Allan, P. Salas, and P. Wahnon, J. Phys. B **23**, 3909 (1990).
[14] H. Croft and A. S. Dickinson, J. Phys. B **29**, 87 (1996).
[15] A. Dubois, S. E. Nielsen, and J. P. Hansen, J. Phys. B **26**, 705 (1993).
[16] W. Gruebler, P. A. Schmelzbach, V. Koening, and P. Marmier, Helv. Phys. Acta **43**, 254 (1970).
[17] T. Nagata, J. Phys. Soc. Jpn. **48**, 2068 (1980).
[18] V. S. Kushawaha, Z. Phys. A **313**, 155 (1983).
[19] K. Berkowitz and J. C. Zorn, Phys. Rev. A **29**, 611 (1984).
[20] F. Aumayr, G. Latikis, and R. Winter, J. Phys. B **20**, 2025 (1987).
[21] J. N. Bardsley, Case Stud. At. Phys. **4**, 299 (1974).
[22] W. R. Thorson and J. B. Delos, Phys. Rev. A **18**, 135 (1978).
[23] T. G. Heil, S. E. Butler, and A. Dalgarno, Phys. Rev. A **23**, 1100 (1981).
[24] B. R. Johnson, J. Comput. Phys. **13**, 445 (1973).
[25] C. E. Moore, *Atomic Energy Levels*, Natl. Bur. Stand. (U.S.), Circ. No. 467 (U.S. GPO, Washington, D.C., 1949), Vol. 1.